

Influence of the degree of atomic ordering on the ferroelectric properties of GaInP₂ solid solutions

© A.S. Vlasov¹, A. Mintairov¹, A.V. Ankudinov¹, N.A. N.Bert¹, N.A. Kalyuzhnyy¹,
D.V. Lebedev¹, R.A. Salii¹, E.V. Pirogov², A.M. Mintairov¹

¹ Ioffe Institute,

St. Petersburg, Russia

² Alferov Academic University, 8 Khlopina, St. Petersburg, Russia

St. Petersburg, Russia

e-mail: vlasov@scell.ioffe.ru

Received May 03, 2024

Revised June 28, 2024

Accepted October 30, 2024

GaInP₂ layers grown by metal-organic epitaxy on GaAs (100) substrates at a temperature of 720°C, V/III group flux ratio of 15–150 and substrate misorientation of 0 and 6° have been investigated. Structural (X-ray diffraction, transmission electron microscopy and Raman-scattering spectroscopy) and optical (photoluminescence) properties together with surface potential measurements (Kelvin probe microscopy) of 500 nm thick layers have been performed. The presence of atomic ordering with CuPt_B structure corresponding to the monolayer superlattice GaP₁/InP₁ along the [111]_B direction and the variation of the degree of ordering $\eta = 0.05 - 0.56$ depending on the growth conditions were shown. Surface potential measurements revealed a decrease in the built-in electric field, suppression of lattice relaxation due to the different symmetry of the substrate and layer (martensitic transition), and fixation (pinning) of the Fermi level as η decreases, which shows the possibility to control the ferroelectric properties of atomically ordered GaInP₂ layers.

Keywords: GaInP₂, Kelvin probe microscopy, atomic ordering, piezoelectric effects.

DOI: 10.61011/EOS.2024.11.60307.6501-24

Introduction

In semiconductor solid solutions Ga_{0.52}In_{0.48}P/GaAs (abbreviated GaInP₂) grown by metal-organic epitaxy under certain epitaxial growth conditions (temperature, substrate orientation, group V/III flux ratio, and etc.), Ga and In atoms can be ordered to form a monolayer superlattice structure (layer alternation) GaP₁-InP₁ in the [111]_B direction (CuPt_B structure) [1,2]. In atomically ordered (AO) GaInP₂ epitaxial layers, the degree of ordering η equal to the fraction of CuPt_B configurations in (111)_B monolayers, reaches 0.6, and the observed microstructure consists of AO domains of size 5–500 nm [3–6]. The CuPt_B ordering corresponds to the rhombohedral crystal structure and the formation of AO domains leads to a change in the electronic properties of the GaInP₂ layers, namely, a decrease in the width of the bandgap and splitting of the valence band, which is important to consider when using the materials in devices [3–6]. Formation of the rhombohedral structure leads to the generation of a built-in electric field (E_{PE}) [6,7], i.e. GaInP₂^{CuPtB} can be referred to as a ferroelectric, which provides an opportunity to use these materials in the structures of quantum gates [8,9]. We have made a detailed analysis of the built-in electric fields of GaInP₂^{CuPtB} layers with a high ordering degree ($\eta \sim 0.5$) and shown that in these layers the values of E_{PE} vary within the range of ± 100 kV/cm and strongly decrease as the layer thickness increases, which is due to the effects of AO domain

relaxation (martensitic transition), Fermi level pinning, and piezoelectric doping [6]. In this study, E_{PE} is measured over a wider range of $\eta \sim 0.05 - 0.56$, including weakly ordered layers ($\eta < 0.3$), which show suppression of the built-in electric field and related effects in GaInP₂^{CuPtB} as η decreases.

Experiment

A detailed description of the conditions for growing GaInP₂^{CuPtB} layers and measurement techniques is given in the preliminary studies of strongly ordered [6] layers. In this study, a method of reducing the V/III flux ratio (to 15) and GaAs substrates (001) misoriented 6° toward the [111] direction were used to vary the degree of ordering η . The thickness of the layers was 500 nm.

The composition of the solid solution x_{In} was determined from X-ray diffraction measurements. The presence of ordering was determined by transmission electron microscopy (TEM) by the presence of superstructure reflections at the positions of $1/2 \{111\}$, corresponding to CuPt_B type and Raman light scattering spectroscopy in terms of anisotropy intensity ($I_{x'x'} - I_{y'y'}$), where $x' \parallel [1-10]$, $y' \parallel [110]$ in the frequency region of InP-type optical phonons (TO₂, LO₂), GaP-type (LO₁) and antiphase boundary (Y) oscillations.

The degree of ordering η was determined from the narrowing of the bandgap width ΔE_g in photoluminescence

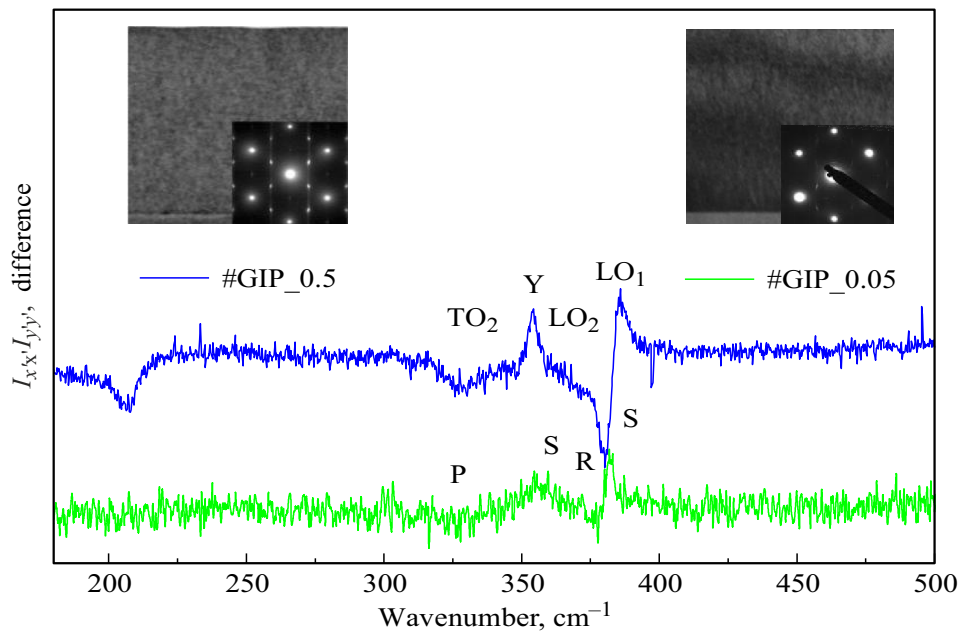


Figure 1. Difference spectra ($I_{x'x'} - I_{y'y'}$) of Raman scattering of samples #GIP_{0.5} and #GIP_{0.05}; insets — bright-field TEM images in the reflection [002] and $[\bar{1}10]$, diffraction pattern (bottom right), #GIP_{0.5} — on the left, #GIP_{0.05} — on the right.

(PL) spectra. Changes in both the flux ratio and substrate misorientation lead to changes in the solid solution composition. To estimate the ordering degree, we traditionally used the method proposed in [10], according to which the bandgap is corrected using the formula

$$E_g^{\text{PL}}(x \rightarrow x_0) = E_g^{\text{PL}} - (x - x_0) \frac{dE_g}{dx},$$

where x — the composition of the investigated layer GaInP₂, x_0 — the composition of the lattice matched one GaInP₂. The ordering degree was calculated according to the formula $\eta = \sqrt{\Delta E_g - \Delta_1}$, where $\Delta_1 = -0.32$ eV [4].

The surface potential was measured using the Kelvin probe microscopy (KPM) technique. $U^{001}(x, y)$ growth plane surface potential maps were measured for several different samples chipped out from each structure's wafer. The presence of martensitic transition and lattice relaxation was determined from sample-to-sample variations of $U^{001}(x, y)$. The electric field strength was calculated by the formula

$$E_{\text{PE}} = (U_0^{001} - U_{\text{GaAs}})/d,$$

where $d = 500$ nm — the thickness of the layer GaInP₂, U_0^{001} — the surface potential of the layer GaInP₂ and U_{GaAs} the surface potential of the substrate n -GaAs. Value U_{GaAs} was measured in KPM maps of the $U^{-110}(z, y)$ sample chip and was equal to 1.1 V at 0° misorientation and 0.6 V at 6° misorientation.

Results

The measured parameters of the investigated samples x_{In} , flux ratio of group V and group III sources $\alpha_{\text{V/III}}$, substrate

Layer parameters GaInP₂ ($d = 500$ nm)

Sample	#GIP _{0.05}	#GIP _{0.1}	#GIP _{0.3}	#GIP _{0.5}
x_{In} , %	48.0	47.3	48.8	45.5
$\alpha_{\text{V/III}}$	15	50	15	150
θ , °	6	6	0	0
ΔE_g , meV	2	4	31	100
η	0.05	0.11	0.31	0.56

misorientation angle θ , ΔE_g and η are shown in the table. The table shows that for $\theta = 0^\circ$ decreasing the flux ratio $\alpha_{\text{V/III}}$ from 150 to 15 results in a decrease in η from $\eta = 0.56$ to 0.31, and for $\alpha_{\text{V/III}} = 50$ the change of θ from 0 to 6° results in a decrease in η from 0.31 to 0.11. The combination of minimum $\alpha_{\text{V/III}} = 15$ and substrates $\theta = 6^\circ$ yields the minimum degree of ordering $\eta = 0.05$.

Fig. 1 shows a comparison of difference Raman spectra ($I_{x'x'} - I_{y'y'}$), samples #GIP_{0.5} and #GIP_{0.05}, reflecting the suppression of the vibrational mode intensity of the antiphase boundary Y (~ 350 cm⁻¹) in the Raman scattering spectra of the weakly ordered sample. The inset of Fig. 1 shows bright-field TEM images of the [002] reflection and electron diffraction images along the axis of the zone $[\bar{1}10]$. Bright-field TEM images show homogeneous contrast, with a slight vertical modulation apparently due to 6° — substrate misorientation. Electron diffraction images show suppression of the $1/2\{111\}$ superstructural reflexes

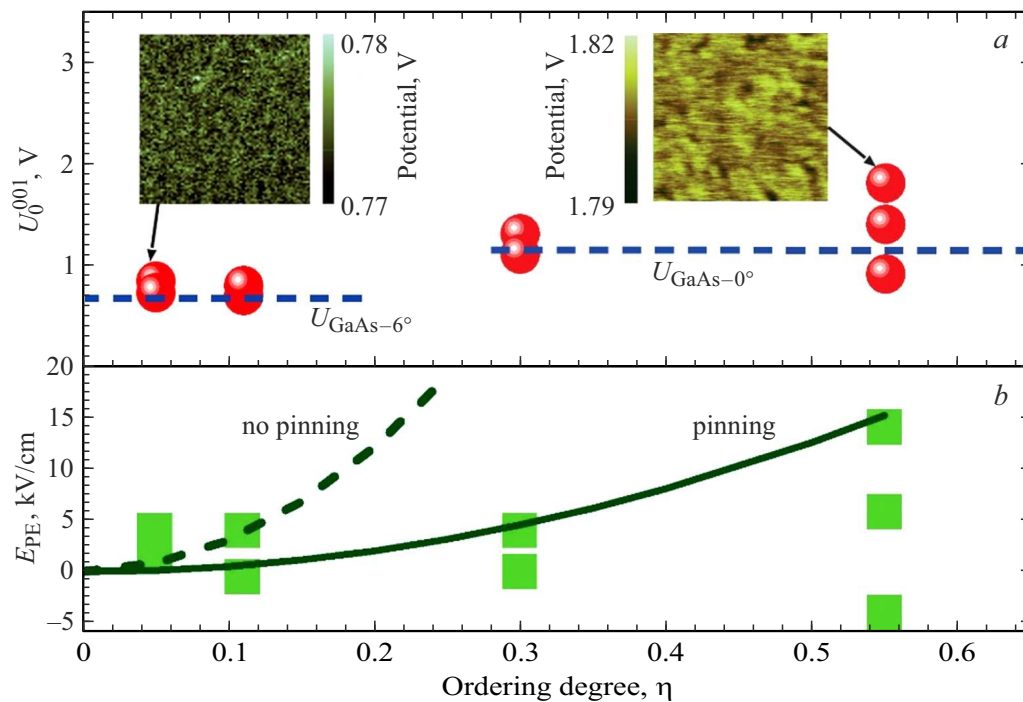


Figure 2. Dependence of surface potential U_0^{001} (a — circles) and built-in electric field strength E_{PE} (b — squares) of GaInP₂ layers on the degree of ordering η . The data for each layer are shown for several samples. The horizontal dashed curves on (a) — GaAs sublayer potentials. The top insets at (a) show the KPM maps of $U^{001}(x, y)$ samples #GIP_{0.05} (left) and #GIP_{0.5} (right). The curve at (b) — approximation of $E_{\text{PE}}(\eta^2)$ with (solid) and without (dashed) Fermi level pinning [8].

for the #GIP_{0.05} sample, consistent with suppression of the Y-mode in this sample.

Fig. 2 shows the surface potential U_0^{001} and the built-in field E_{PE} values of the layers measured for several samples of the same layer. The top insets of Fig. 2, a show KPM maps of the $U^{001}(x, y)$ potential of the #GIP_{0.05} and #GIP_{0.5} samples. As can be seen from the maps, the surface potential of the weakly ordered sample #GIP_{0.05} has spatial variations $\Delta U^{001} \sim 0.01$ V, that are due to instrument noise and a constant „background“ $U_0^{001} = 0.77$ V. In the strongly ordered sample #GIP_{0.5} the potential topography has pits of about 200 nm in size and $\Delta U^{001} \sim 0.03$ V in depth due to AO domains, as shown in [6]. In this sample, $U_0^{001} = 1.8$ V, which is more than twice as large as for #GIP_{0.05} and is due to the larger U_{GaAs} and E_{PE} . Fig. 2, a shows that there is a scatter of η values for different samples with the same U_0^{001} , due to different relaxation of AO domains when the sample is chipped out, i.e., the martensitic transition [6]. This spread ΔU_0^{mart} is ~ 0.2 V for $\eta \leq 0.3$ and ~ 1 V for $\eta = 0.56$. The reduction of ΔU_0^{mart} by a factor of five in weakly ordered samples indicates the suppression of lattice relaxation and martensitic transition. Value ΔU_0^{mart} determines the spread of E_{PE} , and for $\eta = 0.56$ values of fields E_{PE} from -4 to $+14$ kV/cm are observed. As shown in [6], these values correspond to relaxed and stressed states in which the ordered domain atoms are in rhombohedral and cubic configurations, respectively. These values are five to ten times smaller than those observed

for the thin layer ($d = 70$ nm), which is due to Fermi level pinning and relaxation suppression [6]. For $\eta = 0.3$ the expected decrease of E_{PE} to 4 kV/cm (proportional to η^2 [3,4], Fig. 2, b) for the stressed state and suppression of the relaxed state ($E_{\text{PE}} = 0$) are observed. For $\eta = 0.1$ and 0.05 value $E_{\text{PE}} = 4$ kV/cm is also observed, which is several times higher than expected considering the Fermi level pinning. This indicates the suppression of the Fermi level pinning (Fig. 2, b) due to the suppression of the ferroelectric properties.

It should also be noted that the dependence of the built-in field on the relaxation of AO domains and layer thickness can serve as an indirect confirmation of the presence of hysteresis, which is one of the key properties of ferroelectrics.

Conclusion

The dependence of the built-in electric field E_{PE} and martensitic transition of CuPt_B AO layers of GaInP₂ solid solutions on the degree of ordering $\eta = 0.05 - 0.56$ has been investigated by the KPM method. The suppression of E_{PE} , martensitic transition and Fermi level pinning in weakly ordered ($\eta < 0.3$) GaInP₂ has been shown. The results show the possibility of controlling the ferroelectric properties and related effects in the AO layers of GaInP₂.

Funding

This study was supported by the Russian Science Foundation (grant No. 24-29-00375).

Conflict of interest

The authors declare that they have no conflict of interest.

References

- [1] P. Bellon, J.P. Chevalier, G.P. Martin, E. Dupont Nivet, C. Thiebaut, J.P. Andre. *Appl. Phys. Lett.*, **52**, 567 (1988).
- [2] A. Gomyo, T. Suzuki, S. Iijima. *Phys. Rev. Lett.*, **60**, 2645 (1988).
- [3] *Spontaneous ordering in semiconductor alloys* (Springer Science+Business Media, N.Y., 2002).
- [4] A. Zunger, S. Mahajan. *Handbook on Semiconductors* (Elsevier, Amsterdam, 1994). V. 3A.
- [5] C.S. Jiang, H.R. Moutinho, D.J. Friedman, J.F. Geisz, M.M. Al-Jassim. *J. Appl. Phys.*, **93**, 10035 (2003).
- [6] A.V. Ankudinov, N.A. Bert, M.S. Dunaevskiy, A.I. Galimov, N.A. Kalyuzhnyy, S.A. Mintairov, A.V. Myasoedov, N.V. Pavlov, M.V. Rakhlin, R.A. Salii, A.A. Toropov, A.S. Vlasov, E.V. Pirogov, M.A. Zhukovskiy, A.M. Mintairov. *Appl. Phys. Lett.*, **124**, 052101 (2024).
- [7] S. Froyen, A. Zunger, A. Mascarenhas. *Phys. Rev. B*, **53**, 4570 (1996).
- [8] A.M. Mintairov, A.V. Ankudinov, N.A. Kalyuzhnyy, D.V. Lebedev, S.A. Mintairov, N.V. Pavlov, A.I. Galimov, M.V. Rakhlin, R.A. Salii, A.A. Toropov, A.S. Vlasov, D. Baretin, M. Auf der Maur, S.A. Blundell. *Appl. Phys. Lett.*, **118**, 121101 (2021).
- [9] P.A. Balunov, A.V. Ankudinov, I.D. Breev, M.S. Dunaevskiy, A.S. Goltaev, A.I. Galimov, V.N. Jmerik, K.V. Likhachev, M.V. Rakhlin, A.A. Toropov, A.S. Vlasov, A.M. Mintairov. *Appl. Phys. Lett.*, **122**, 222102 (2023).
- [10] T. Suzuki, A. Gomyo, S. Iijima, K. Kobayashi, S. Kawata, I. Hino, T. Yuasa. *Jpn. J. Appl. Phys.*, **27**, 2098 (1988).

Translated by J.Savelyeva